Heliyon 7 (2021) e06227

Contents lists available at ScienceDirect

Heliyon

journal homepage: www.cell.com/heliyon

Research article

Design, synthesis and evaluation of novel enzalutamide analogues as potential anticancer agents

Ritesh P. Bhole [a,*], Rupesh V. Chikhale [b,c], Ravindra D. Wavhale [a], Fatmah Ali Asmary [d], Tahani Mazyad Almutairi [d], Hassna Mohammed Alhajri [d], Chandrakant G. Bonde [e]

[a] Dr. D. Y. Patil Institute of Pharmaceutical Sciences and Research, Pimpri, Pune 411018, Maharashtra, India
[b] Division of Pharmacy and Optometry, University of Manchester, Manchester, UK
[c] School of Pharmacy, University of East Anglia, Norwich, UK
[d] Department of Chemistry, P.O. Box 2455, College of Science, King Saud University, Riyadh, 11451, Saudi Arabia
[e] School of Pharmacy & Technology Management, SVKM's NarseeMonjee Institute of Management & Studies (NMIMS), Mukesh Patel Technology Park, Shirpur, Dhule, 425405, Maharashtra, India

ARTICLE INFO

Keywords:
Hybrid molecules
Prostate cancer
Imidazolidinone derivatives
Molecular docking
Molecular dynamics simulations
Binding energy calculations

ABSTRACT

The androgen receptor inhibitor, Enzalutamide, proved effective against castration resistance prostate cancer, has demonstrated clinical benefits and increased survival rate in men. However, AR mutation (F876L) converts Enzalutamide from antagonist to agonist indicating a rapid evolution of resistance. Hence, our goal is to overcome this resistance mechanism by designing and developing novel Enzalutamide analogues. We designed a dataset of Enzalutamide derivatives using Enzalutamide's shape and electrostatic features to match with pharmacophoric features essential for tight binding with the androgen receptor. Based on this design strategy ten novel derivatives were selected including 5,5-dimethyl-3-(6-substituted benzo[d]thia/oxazol-2-yl)-2-thioxo-1-(4-(trifluoromethyl) pyridin-2-yl)imidazolidin-4-one (**6a-j**) for synthesis. All the compounds were evaluated *in-vitro* on prostate cancer cell lines DU-145, LNCaP and PC3. Interestingly, two compounds 3-(6-hydroxybenzo[d]thiazol-2-yl)-5,5-dimethyl-2-thioxo-1-(4-(trifluoromethyl)pyridin-2-yl) imidazolidin-4-one (**6c**, IC_{50} – 18.26 to 20.31μM) and 3-(6-hydroxybenzo[d]oxazol-2-yl)-5,5-dimethyl -2-thioxo- 1- (4-(trifluoromethyl) pyridin-2-yl)imidazolidin-4-one (**6h**, IC_{50} – 18.26 to 20.31μM) were successful with promising *in-vitro* antiproliferative activity against prostate cancer cell lines. The binding mechanism of potential androgen receptor inhibitors was further studied by molecular docking, molecular dynamics simulations and MM-GBSA binding free energy calculations and found in agreement with the *in vitro* studies. It provided strong theoretical support to our hypothesis.

1. Introduction

Prostate cancer is the cancer of prostate gland in the male reproductive system, which is the second most frequent cancer in men and fifth amongst all cancer mortality. According to the World Health Organization report, in 2018, 1.28 million new prostate cancer cases were found of 18.1 million cancer cases, worldwide [1]. Prostate cancer is generally observed in older age patients with asymptomatic during the early stage. Later, most common complaints are difficulty in urination, blood in urine and pain in pelvis or back. Treatment strategies of prostate cancer are based on lowering the male sex hormone levels called testosterone, as it plays a central role in cancer growth. Testosterone level can be reduced either by surgical castration [2] (removal of testicles) or by testosterone lowering agents (Androgen deprivation therapy or ADT). ADT includes steroidal or nonsteroidal drugs like Luteinizing Hormone, Releasing hormone agonist and antagonist that reduces blood testosterone levels or Androgen receptor inhibitors, which block testosterone's entry in the cell (cancer cell). Competitive Inhibition of androgen binding to the androgen receptors (AR) using AR antagonists like Flutamide, Nilutamide, and Bicalutamide (First generation AR antagonists) reduces androgen concentration inside the cell [3]. However, development of resistance due to AR mutations, Synthesis of androgen by prostate cancer cells, overexpression of AR, and AR antagonists' turning to agonists makes these conventional AR antagonists ineffective in treating castration-resistant prostate cancer (CRPC) [4].

* Corresponding author.
E-mail address: ritesh.bhole@dypvp.edu.in (R.P. Bhole).

https://doi.org/10.1016/j.heliyon.2021.e06227
Received 20 September 2020; Received in revised form 13 January 2021; Accepted 4 February 2021

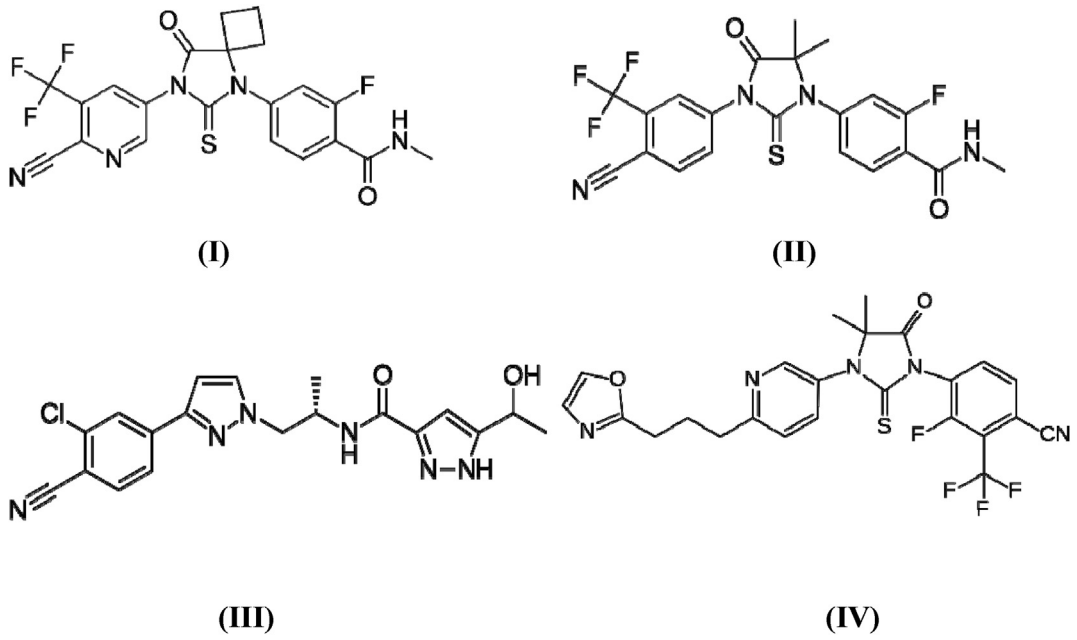

Figure 1. Representative second-generation AR antagonists.

CRPC is the most aggressive and incurable form of prostate cancer where the tumour keeps growing even with deficient testosterone in the body. Recently developed next-generation AR antagonists (Figure 1) Apalutamide (I), Enzalutamide (II) (FDA approved), Darolutamide (III) and Proxalutamide (IV) (under clinical trials) increased the hopes of overall survival for patients with CRPC [5].

Enzalutamide is the most promising option for treating deadly CRPS. It is a nonsteroidal androgen receptor inhibitor with five to eight-fold higher affinity than clinically used bicalutamide effective in metastatic and non-metastatic CRPS [6]. Enzalutamide also impacts the nuclear translocation of AR and prevents AR binding to deoxyribonucleic acid (DNA) and co-activator proteins [7].However, current findings revealed that the F876L mutation in AR leads to the genetic and phenotypic changes indicating rapid evolution of drug resistance [8].Recently Bassetto et al., reported developing some novel bicalutamide and enzalutamide derivatives as antiproliferative agents in treating prostate cancer. Synthesised novel fluorinated analogues of bicalutamide and enzalutamide and found a 50-fold improvement in the activity. These compounds also showed a full AR antagonist effect. However, there are very few research works published that address this problem. Hence, it's an urgent and unmet need to overcome this resistance mechanism by designing and developing novel Enzalutamide analogues to treat CRPC successfully. Here, we demonstrated a hypothesis by designing a small dataset of enzalutamide analogues by achieving 3D shape and electrostatic similarity studies. Top ten Tanimoto scoring molecules as 5,5-dimethyl-3-(6--substituted-benzo[d]thia/oxazol-2-yl)-2-thioxo-1-(4-(trifluoromethyl) pyridin-2-yl)imidazolidin-4-ones (**6a-j**) were selected for synthesis and evaluated in-*vitro* against prostate cancer cell lines DU-145, LNCaP and PC3. Mechanism of active candidates was further studied by molecular docking, molecular dynamics simulations and MM-GBSA binding free energy calculations. In-silico results found to be in agreement with the *in vitro* studies and provide insights for further exploration of active HITs.

2. Experimental

2.1. Design of novel AR antagonists

All the molecular docking studies were carried out on the Schrodinger molecular modelling suite (Maestro, version 9.0 and 9.4) and academic visualiser of Maestro 19.2, the modules used were Ligprep, Protein preparation wizard and Glide [9]. MD studies carried out on the pre and post-synthetic modes. In the first step, all the molecules designed were subjected to various confirmations and minimisation of energies, done using the Limper module; it optimises all the energies and provides all possible confirmations for a particular molecule. These are stored in the module's worktable and subjected to docking.

The protein structure (PDB: 3V49) contains cofactors, water molecules and several other groups needed to form a crystal. In protein preparation, water molecules and ions were removed using the protein preparation wizard [10]. The grid was generated using the receptor grid generation panel. The molecular docking was carried out with a Glide module of software; compounds were docked on the prepared protein. All the simulations were done on the OPLS5.0 force field with the molecules flexible and ten conformations allowed each molecule in the standard precision (XP) mode. The AR crystal structure (PDB 3V49) was employed as the receptor with compounds **6a-j** as ligands.[14]The results obtained in the form of dock score representing the minimum energies, the interaction between the ligand and the respective residues also presented. H-bond, van der Waals forces reported as well.

3. Material and methods

3.1. General

The chemicals and solvents used in this work obtained from Alfa Aeser, UK and Sigma Aldrich, USA. Melting points (mp) for all the compounds was carried out within open capillaries using Theil's tube melting-point device and recorded uncorrected. IR spectra (KBr) were developed and created on JASCO FT/IR-4000 spectrophotometer (Jasco, USA). ^{1}H spectra were obtained from a Bruker Advance-II 400 Spectrometer on 400 MHz using tetramethylsilane (TMS) as the internal standard. The chemical shift values for all the synthetic derivatives recorded as δ (parts per million). Coupling constant value J measured in hertz. The peaks are presented as s = singlet, d = doublet, t = triplet, dd = double doublet, m = multiple. TLC method used to determine the purity of compounds using Merck, silica gel, HF254–361, type 6, 0.25 mm. Electron Spray Ionization Mass Spectrometry recorded on Waters HPLC system with Q-Time of Flight LC-MS spectrometry (Waters-Micromass LC-MS, US).

3.2. Molecular modelling studies

Crystal structures from the Research Collaboratory for Structural Bioinformatics Protein Data Bank (RCSB-PDB) selected for molecular docking study. Androgen receptor crystal structure (PDB ID: 3V49) was chosen; as this crystal structure have a known active site with bound Enzalutamide [11].The protein preparation wizard of Schrödinger maestro v9.0 was used to prepare the receptor protein by adding hydrogen, treating metal, deleting water molecules and assigning partial charges by using the OPLS-2005 force field, then setting protonation states and determining restrained and further partial energy minimised with 0.3Å RMSD limit. The binding site was defined by referring the ligand then grid generated using a grid box volume of 20_20_20 Å. The shape similarity analysis was also carried out and results were shown in Table 1.

The dataset of ten experimental compounds, enzalutamide (ENZ), bicalutamide (BIC) with their possible conformations were exported in Schrodinger Maestro v9.0 (Schrödinger, Inc., New York, NY). Each structure subsequently processed with the LigPrep v2.3 (Schrödinger, Inc., New York, NY) to assign protonation states appropriate for physiological pH, using the "ioniser" subprogram. Ligand structures obtained from the LigPrep run used for generating 32 ligand conformations using the default parameters of mixed torsional/Low-mode sampling function.

Molecular docking performed by extra precision (XP) method using the Glide module of the Schrodinger Suite. The lowest energy binding pose of each docked ligand retained. The docking experiment results were analysed using glide XP visualiser, and the crucial active site interactions recorded along with the scoring functions.

All ten ligands, ENZ and BIC, docked complexes simulated using AMBER18 package [12, 13] Topology and coordinate parameters for androgen receptor generated with an AMBER99SB force field. The ligands were parametrised with a general amber force field (GAFF)in the xLeap module. The ligand parametrisation performed with ANTECHAMBR [14] program in the AMBER18package. The protein-ligand complexes embedded in the TIP3P water model with a margin of 1.0 nm in a periodic cubic box [15]. The system was neutralised to pH seven by adding counter ions. Added a sufficient number of ions to obtain the salt concentration of 1.5 M. All the bond lengths were constrained using the SHAKE algorithm, and electrostatic interactions were calculated by the Particle Mesh Ewald (PME) method. The solvated system was subjected to energy minimisation using the steepest descent algorithm to eliminate bad contacts with added water molecules until a series of equilibration protocol reached a tolerance of 1000 kJ mol-1. The system was further treated for equilibration by five ns NVT simulation at 300 K, followed by five ns of NPT simulation to achieve the simulated system's proper equilibration. Final production simulations were performed in the isothermal isobaric (NPT) ensemble at 300 K, using an external bath with a coupling constant of 0.1 ps, the total simulation time achieved was 100 ns. Using pressure coupling pressure was kept constant (1 bar) with the time constant to 1 ps. The trajectories stored at every two ps during the simulation and trajectories analysed using built-in commands of AMBER18. Trajectories of docked complexes used to calculate binding energies using Van der Waal, electrostatic, polar solvation, SASA, and Schrodinger binding and docking with protein carried out using Glide docking module. The molecular mechanics generalised Born surface area (MM-GBSA) method AMBER18 was used to measure the receptor and ligands' binding strength quantitatively [16]. The average interaction energies of all the ten compounds, BIC and ENZ, was calculated for 100 ns of MD trajectories [13].

3.3. Chemistry

To obtain the final products compounds **6a-j**, the four-step synthetic protocol was followed, initially compound **2a-j** were prepared from compounds **1a-j**. Simultaneously, compound **3, 4** were synthesised and finally in the cyclisation step final derivatives **6a-j** were synthesised and characterised. Detailed Synthesis is discussed below as follows; Procedure for Synthesis of 2-isothiocyanato-6-substituted benzo[d]thiazole **2a-j**.

Substituted 2-amino benzothiazoles/benzoxazoles**1a-j** (1.0 mmol) were added to a mixture of DMF (5 mL) & $NaHCO_3$ (0.82 g) in water (5 mL), the resultant solution was cooled to -5 °C, to this cold solution thiophosgene (3.8 mmol) was added dropwise with stirring, the addition was completed in 10 min, after that the mixture was stirred overnight. The resulting mixture was extracted with DCM (20 mL x 2) and wash with a solution of NaCl (Saturated); the organic layer was separated and dried over Na_2SO_4 and concentrated under vacuum to obtain the products.

3.3.1. Procedure for Synthesis of 2-methyl-2-(4-(trifluoromethyl)pyridin-2-ylamino) propanoic acid *4*

2-Bromo-4-(trifluoromethyl)pyridine**3** (5.95 mmol) was added to a blend of DMF: Water (9:1) (10 mL), this solution was added to a mixture of K_2CO_3 (18.0mmol), CuCl (1.5 mmol) and 2-aminoisobutyric acid (10.0 mmol). The reaction mixture was warmed to 30 °C, and then 2-acetylcycloheanone (1.40 mmol) was added. The reaction mixture was stirred overnight at 120 °C. On cooling, the reaction mixture was extracted with water (20 × 2 mL) and ethyl acetate (20 × 2 mL). The organic solvent was dried over Na_2SO_4 and concentrated under vacuum to obtain compound **4**.

3.3.2. Procedure for Synthesis of methyl 2-methyl-2-(4-(trifluoromethyl) pyridin-2-ylamino)propanoate *5*

A mixture of **4** (10 mmol) in a solution of K_2CO_3 (8.5 mmol) and DMF:Water (7:3) (10 mL) was warmed to 30 °C. To this mixture Iodomethane (10 mmol) was added and heated to 40 °C for 2–3 h. To this solution, dilute acetic acid (0.144 mL) was added. The reaction mixture was allowed to cool and extracted with DCM (20 × 2 mL), dried over Na_2SO_4. The organic layer was concentrated under vacuum to provide with the product in quantitative yield.

3.3.3. Procedure for Synthesis of 5,5-dimethyl-3-(6-methylbenzo[d]thiazol-2-yl)-2-thioxo-1- (4-(trifluoromethyl) pyridin-2-yl)imidazolidin-4-one *6a*

A mixture of **2a** (2.0 mmol) and **5** (2.0 mmol) was dissolved in a mixture of DMSO: Isopropyl acetate (1:2) (10 mL) and stirred overnight at 84 °C. The reaction mixture was then extracted with EtOAc and washed with brine. The organic layer was dried over $MgSO_4$ and concentrated under vacuum to obtain the final derivative as **6a.**

Mp:256–258 °C; ^{1}H NMR ($CDCl_3$): δ 1.34 (s, 6H, CH_3), 2.36 (s, 3H, CH_3), 6.62 (m, 1H, Ar–H), 6.7 (d, 1H, J = 6.8, Ar–H), 7.35 (m, 1H, Ar–H), 7.92 (s, 1H, Ar–H), 8.11 (s, 2H, Ar–H);^{13}C-NMR ($CDCl_3$): δ 177.0, 171.4, 160.0, 155.5, 153.2, 150.2, 147.3,134.1, 148.8, 130.7, 126.6, 123.6, 121.3, 117.7, 123.6, 124.1, 112.7, 23.4(2); Anal. Calcd for $C_{19}H_{15}F_3N_4OS_2$: C, 52.28; H, 3.46; F, 13.06; N, 12.84; O, 3.67; S, 14.69; MS (ESI) m/z:436.0639.

3.3.4. Procedure for Synthesis of 3-(6-methoxybenzo[d]thiazol-2-yl)-5,5-dimethyl-2-thioxo-1-(4-(trifluoromethyl)pyridin-2-yl)imidazolidin-4-one *6b*

A mixture of **2b** (2.0 mmol) and **5** (2.0 mmol) was dissolved in a mixture of DMSO: Isopropyl acetate (1:2) (10 mL) and stirred overnight at 84 °C. The reaction mixture was then extracted with EtOAc and washed with a concentrated solution of NaCl. The organic layer was dried over $MgSO_4$ and concentrated under vacuum to obtain the final derivative as **6b**.

Mp: 259–261 °C; ^{1}H-NMR ($CDCl_3$): δ 1.37 (s, 6H, CH_3), 3.73 (s, 3H, O–CH_3), 6.67 (m, 1H, Ar–H), 6.86 (d, 1H, J = 6.87, Ar–H), 7.19 (m, 1H, Ar–H), 7.56 (s, 1H, Ar–H), 8.15 (s, 2H, Ar–H); ^{13}C-NMR ($CDCl_3$): δ 160.0, 171.4, 177.0, 145.5, 78.4, 156.7, 153.2, 147.3, 104.9, 118.2, 148.8, 112.7, 114.6, 117.7, 124.1, 55.8, 23.1(2); Anal. Calcd for

Table 1. The ROCS Tanimoto shape similarity coefficient (TSSC), Tanimotocolor similarity coefficient (TCSC) and Tanimoto combine (TC) of compounds 6a-6j with respect to the structure of Enzalutamide.

Data set	6a	6b	6c	6d	6e	6f	6g	6h	6i	6j
TSSC	0.669	0.572	0.676	0.567	0.58	0.587	0.671	0.671	0.646	0.677
TCSC	0.413	0.434	0.404	0.354	0.413	0.407	0.381	0.381	0.362	0.408
TC	1.082	1.007	1.08	0.92	0.993	0.994	1.052	1.052	1.008	1.084

$C_{19}H_{15}F_3N_4O_2S_2$: C, 50.43; H, 3.34; F, 12.60; N, 12.38; O, 7.07; S, 14.17; MS (ESI) m/z:452.0589.

3.3.5. Procedure for Synthesis of 3-(6-hydroxybenzo[d]thiazol-2-yl)-5,5-dimethyl-2-thioxo-1-(4-(trifluoromethyl)pyridin-2-yl)imidazolidin-4-one **6c**

A mixture of **2c** (2.0 mmol) and **5** (2.0 mmol) was dissolved in a mixture of DMSO: Isopropyl acetate (1:2) (10 mL) and stirred overnight at 84 °C. The reaction mixture was extracted with EtOAc and brine. The isolated organic layer was dried over $MgSO_4$ and concentrated under vacuum to obtain the final derivative as **6c**.

Mp: 239–241 °C; ^{1}H-NMR ($CDCl_3$): δ 1.24 (s, 6H, CH_3), 6.5 (m, 1H, Ar–H), 6.76 (d, 1H, J = 6.82, Ar–H), 7.20 (m, 1H, Ar–H), 7.74 (s, 1H, Ar–H), 8.01 (s, 2H, Ar–H), 11.3 (s, 1H, Ar-OH);^{13}C-NMR ($CDCl_3$): δ 160.0, 132.3, 171.4, 177.0, 145.8, 78.4, 155.1, 153.2, 147.3, 106.5, 117.9, 148.8, 112.7, 114.9, 117.7, 124.1, 23.7(2); Anal. Calcd for $C_{18}H_{13}F_3N_4O_2S_2$: C, 49.31; H, 2.99; F, 13.00; N, 12.78; O, 7.30; S, 14.63; MS (ESI) m/z:438.0432.

3.3.6. Procedure for Synthesis of 5,5-dimethyl-3-(6-nitrobenzo[d]thiazol-2-yl)-2-thioxo-1-(4-(trifluoromethyl)pyridin-2-yl)imidazolidin-4-one **6d**

A mixture of **2d** (2.0 mmol) and **5** (2.0 mmol) was dissolved in a mixture of DMSO: Isopropyl acetate (1:2) (10 mL) and stirred overnight at 84 °C. The reaction solvent system was then extracted dichloro methane and washed with brine. The DCM layer was dried over $MgSO_4$ and concentrated under vacuum to obtain the final derivative as **6d**.

Mp:289–290 °C; ^{1}H-NMR ($CDCl_3$): δ 1.73 (s, 6H, CH_3), 6.7 (m, 1H, Ar–H), 6.82 (d, 1H, J = 6.85, Ar–H), 7.22 (m, 1H, Ar–H), 7.73 (s, 1H, Ar–H), 8.19 (s, 2H, Ar–H);^{13}C-NMR ($CDCl_3$): δ 160.6, 131.3, 171.4, 177.0, 159.3, 78.4, 153.2, 147.3, 144.3, 119.1, 117.3, 148.8, 112.7, 121.3, 118.7, 124.3(2); Anal. Calcd for $C_{18}H_{12}F_3N_5O_3S_2$:C, 46.25; H, 2.59; F, 12.19; N, 14.98; O, 10.27; S, 13.72; MS (ESI) m/z:467.0334.

3.3.7. Procedure for Synthesis of 3-(6-chlorobenzo[d]thiazol-2-yl)-5,5-dimethyl-2-thioxo-1-(4-(trifluoromethyl)pyridin-2-yl)imidazolidin-4-one **6e**

A mixture of **2e** (2.0 mmol) and **5** (2.0 mmol) was dissolved in a mixture of DMSO: Isopropyl acetate (1:2) (10 mL) and stirred overnight at 84 °C. The reaction mixture was then extracted with dichlro methane (DCM) and washed with salt water. The organic layer was dried over magnesium sulfate and concentrated under vacuo to obtain the final derivative as **6e**.

Mp: 250–252 °C; ^{1}H-NMR ($CDCl_3$): δ 1.72 (s, 6H, CH_3), 6.3 (m, 1H, Ar–H), 6.43 (d, 1H, J = 6.80, Ar–H), 6.9 (m, 1H, Ar–H), 7.11 (s, 1H, Ar–H), 7.92 (s, 2H, Ar–H);^{13}C-NMR ($CDCl_3$): δ 163.1, 132.3, 171.4, 177.3, 151.3, 78.4, 129.8, 153.2, 147.3, 121.2, 118.3, 148.8, 112.7, 125.8, 117.7, 124.1, 23.1(2); Anal. Calcd for $C_{18}H_{12}ClF_3N_4OS_2$: C, 47.32; H, 2.65; Cl, 7.76; F, 12.47; N, 12.26; O, 3.50; S, 14.04; MS (ESI) m/z:456.0093.

3.3.8. Procedure for Synthesis of 5,5-dimethyl-3-(6-methylbenzo[d]oxazol-2-yl)-2-thioxo-1-(4-(trifluoromethyl)pyridin-2-yl)imidazolidin-4-one **6f**

A mixture of **2f** (2.0 mmol) and **5** (2.0 mmol) was dissolved in a mixture of DMSO: Isopropyl acetate (1:2) (10 mL) and stirred overnight at 84 °C. The reaction mixture was then extracted with DCM and washed with brine. The DCM layer was dried over sodium sulphate and concentrated under vacuum to obtain the final derivative as **6f**.

Table 2. Antiproliferative activity of novel Enzalutamide analogues (**6a - 6j**).

Sr. no.	Compound	IC_{50} (μM)		
		DU145	LNCaP	PC-3
1	**6a**	20.94	17.4	18.52
2	**6b**	22.43	19.32	21.73
3	**6c**	**20.31**	**19.21**	**18.36**
4	**6d**	>100	48.14	59.00
5	**6e**	>100	38.12	59.31
6	**6f**	>100	43.2	49.10
7	**6g**	45.12	35.44	34.74
8	**6h**	**16.50**	**22.41**	**20.44**
9	**6i**	21.34	19.87	23.15
10	**6j**	>100	50.65	68.39
11	**Std**	28.20	31.78	27.32

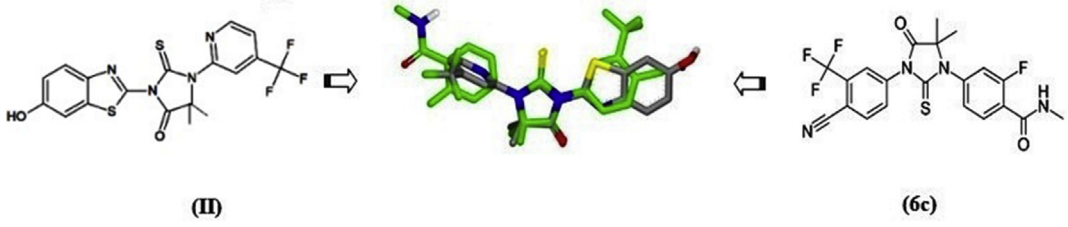

Figure 2. Structural feature and overlay study of Enzalutamide(**II**, Green) with a designed molecule (**6c**, Gray).

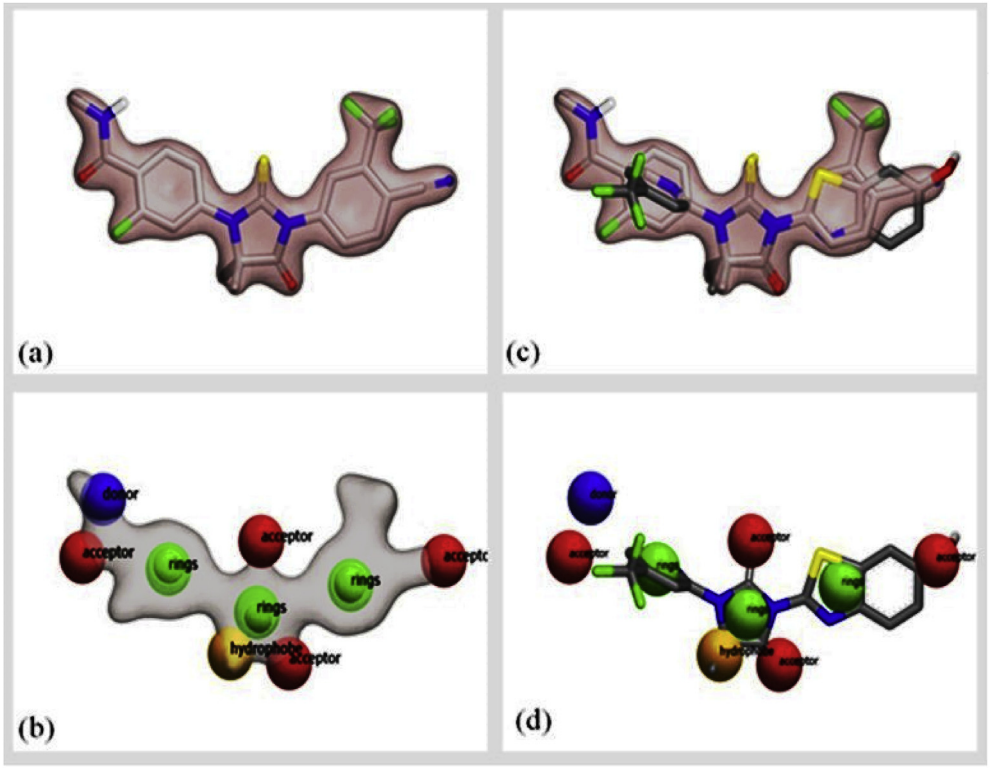

Figure 3. (a) Shape and (b) electrostatic features of ENZ (II). (c) Overlay of the designed compound with ENZ (II) showing similar shape and volume. (d) The electrostatic similarity of the designed compound with ENZ (II).\

Mp: 234–236 °C; ^{1}H-NMR ($CDCl_3$): δ 1.35 (s, 6H, CH_3), 2.39 (s, 3H, CH_3), 6.60 (m, 1H, Ar–H), 6.73 (d, 1H, J = 6.1, Ar–H), 7.32 (m, 1H, Ar–H), 7.91 (s, 1H, Ar–H), 8.15 (s, 2H, Ar–H); ^{13}C-NMR ($CDCl_3$): δ 171.4, 152.6, 149.9, 177.0, 165.6, 78.4, 153.2, 147.3, 111.5, 119.0, 132.2, 148.8, 112.7, 123.6, 126.7, 117.7, 124.1, 23.4(2); Anal. Calcd for $C_{19}H_{15}F_3N_4O_2S$: C, 54.28; H, 3.60; F, 13.56; N, 13.33; O, 7.61; S, 7.63; MS (ESI) m/z:420.0868.

*3.3.9. Procedure for Synthesis of 3-(6-methoxybenzo[d]oxazol-2-yl)-5,5-dimethyl-2-thioxo-1-(4-(trifluoromethyl)pyridin-2-yl)imidazolidin-4-one **6g***

A mixture of **2g** (2.0 mmol) and **5** (2.0 mmol) was dissolved in a mixture of DMSO: Isopropyl acetate (1:2) (10 mL) and stirred overnight at 84 °C. The reaction mixture was then extracted with ethyl acetate and washed with brine. The organic layer was dried over $MgSO_4$ and concentrated under vacuum to obtain the final derivative as **6g**.

Mp: 241–243 °C; ^{1}H-NMR ($CDCl_3$): δ 1.32 (s, 6H, CH_3), 3.78 (s, 3H, O–CH_3), 6.66 (m, 1H, Ar–H), 6.86 (d, 1H, J = 6.80, Ar–H), 7.22 (m, 1H, Ar–H), 7.55 (s, 1H, Ar–H), 8.01 (s, 2H, Ar–H); ^{13}C-NMR ($CDCl_3$): δ 171.4, 152.6, 149.9, 177.0, 140.6, 78.4, 147.3, 111.5, 119.0, 132.2, 148.8, 112.7, 126.7, 117.7, 124.1, 23.3(2), 21.6; Anal. Calcd for $C_{19}H_{15}F_3N_4O_3S$: C, 52.29; H, 3.46; F, 13.06; N, 12.84; O, 11.00; S, 7.35; MS (ESI) m/z:436.0817.

*3.3.10. Procedure for Synthesis of 3-(6-hydroxybenzo[d]oxazol-2-yl)-5,5-dimethyl-2-thioxo-1-(4-(trifluoromethyl)pyridin-2-yl)imidazolidin-4-one **6h***

A mixture of **2h** (2.0 mmol) and **5** (2.0 mmol) was dissolved in a mixture of DMSO: Isopropyl acetate (1:2) (10 mL) and stirred overnight at 84 °C. The reaction mixture was then extracted with DCM and washed with brine. The organic layer was dried over Na_2SO_4 and concentrated under vacuum to obtain the final derivative as **6h**.

Mp: 237–238 °C; ^{1}H-NMR ($CDCl_3$): δ 1.22 (s, 6H, CH_3), 6.52 (m, 1H, Ar–H), 6.77 (d, 1H, J = 6.88, Ar–H), 7.22 (m, 1H, Ar–H), 7.73 (s, 1H, Ar–H), 8.05 (s, 2H, Ar–H), 11.1 (s, 1H, Ar-OH); ^{13}C-NMR ($CDCl_3$): δ 171.4, 152.6, 151.4, 177.0, 136.2, 78.4, 153.2 (2),147.3, 98.0, 120.5, 148.8, 112.7, 116.3, 117.7, 124.1, 23.1(2); Anal. Calcd for $C_{18}H_{13}F_3N_4O_3S$: C, 51.18; H, 3.10; F, 13.49; N, 13.26; O, 11.36; S, 7.59; MS (ESI) m/z:422.0660.

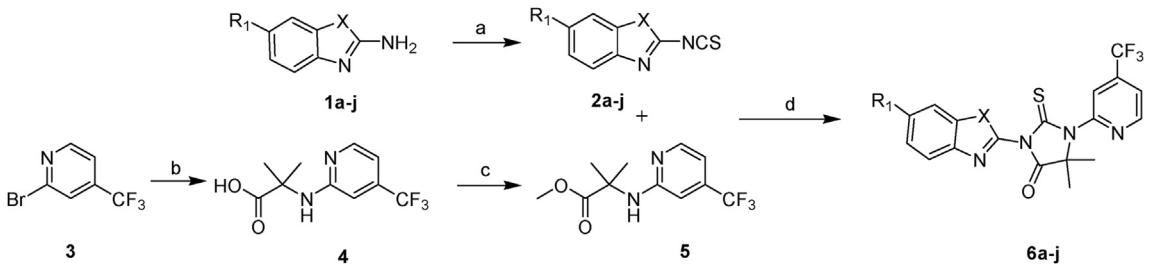

Scheme 1. Synthetic scheme for **6a-6j**; Reagents and conditions: (a) Thiophosgene, $NaHCO_3$; d) DMSO, 2-acetoxypropane. (b) 2-aminoisobutyric acid, K_2CO_3, CuCl, 2-acetylcyclohexanone; (c) Methyl iodide, K_2CO_3; c) Thiophosgene, Sodium hydrogen carbonate, H_2O, Dichloro methane, RT, 24 h; d) Dimethyl Sulphoxide, 2-acetoxypropane.

3.3.11. Procedure for Synthesis of 5,5-dimethyl-3-(6-nitrobenzo[d]oxazol-2-yl)-2-thioxo-1-(4-(trifluoromethyl)pyridin-2-yl)imidazolidin-4-one **6i**

A mixture of **2i** (2.0 mmol) and **5** (2.0 mmol) was dissolved in a mixture of DMSO: Isopropyl acetate (1:2) (10 mL) and stirred overnight at 84 °C. The reaction mixture was then extracted with EtOAc and washed with brine. The acetate layer was dried over $MgSO_4$ and concentrated under vacuum to obtain the final derivative as **6i**.

Mp: 279–281 °C; ^{1}H-NMR ($CDCl_3$): δ 1.72 (s, 6H, CH_3), 6.69 (m, 1H, Ar–H), 6.80 (d, 1H, J = 6.84, Ar–H), 7.20 (m, 1H, Ar–H), 7.71 (s, 1H, Ar–H), 8.12 (s, 2H, Ar–H); ^{13}C-NMR ($CDCl_3$): δ 171.8, 152.6, 147.2, 177.0, 149.7, 78.4, 147.7,144.2, 104.5, 114.1, 148.8, 112.7, 121.3, 117.7, 124.1, 23.9(2); Anal. Calcd for $C_{18}H_{12}F_3N_5O_4S$: C, 47.90; H, 2.68; F, 12.63; N, 15.52; O, 14.18; S, 7.10; MS (ESI) m/z:451.0562.

3.3.12. Procedure for Synthesis of 3-(6-chlorobenzo[d]oxazol-2-yl)-5,5-dimethyl-2-thioxo-1-(4-(trifluoromethyl)pyridin-2-yl)imidazolidin-4-one **6j**

A mixture of **2j** (2.0 mmol) and **5** (2.0 mmol) was dissolved in a mixture of DMSO: Isopropyl acetate (1:2) (10 mL) and stirred overnight at 84 °C. The reaction mixture was then extracted with DCM and washed with brine. The organic layer was dried over Na_2SO_4 and concentrated under vacuum to obtain the final derivative as **6j**.

Mp: 231–233 °C; ^{1}H-NMR ($CDCl_3$): δ 1.71 (s, 6H, CH_3), 6.33 (m, 1H, Ar–H), 6.44 (d, 1H, J = 7.11, Ar–H), 6.89 (m, 1H, Ar–H), 7.01 (s, 1H, Ar–H), 7.90 (s, 2H, Ar–H); ^{13}C-NMR ($CDCl_3$): δ 171.4, 152.6, 151.4, 177.0, 141.7, 78.4, 127.2, 153.2, 147.3, 111.2, 121.5, 148.8, 112.3, 123.7, 118.7, 124.1, 23.7(2); Anal. Calcd for $C_{18}H_{12}ClF_3N_4O_2S$: C, 49.04; H, 2.74; Cl, 8.04; F, 12.93; N, 12.71; O, 7.26; S, 7.27; MS (ESI) m/z:440.0322.

3.4. Biological evaluation

3.4.1. In-vitro studies

3.4.1.1. Cell culture. All the three cell lines were obtained from the ATCC, USA; DU145, LNCaP and PC-3 and were preserved suitably, these were further cultured in the Dulbecco's Eagle medium modified to contain supplements like the fetal Bovine Serum (10%) with penicillin (100 U/mL) and Streptomycin (0.1 mg/mL). These were incubated under 5 % CO_2 at humid conditions with 37 °C temperature.

3.4.1.2. Antiproliferative assay by Oncotest method. The imidazolidinones were assayed for their antiproliferative activity by the Oncotest's monolayer method developed earlier by Maier et. al [17]. against the prostate cancer cell lines. Enzalutamide employed as a standard drug. This assay is based on the propodeum iodide method and the compounds observed after four days of treatment. The results are presented by nonlinear regression analysis as IC_{50} in Table 2. All the ten derivative **6a-j** were evaluated at ten dilutions with a half-log increase up to the 100 1M in triplicates [18, 19, 20, 21, 22, 23, 24].

3.4.1.3. Oncotest protocol and its modifications. A modified Propidium Iodideassay was used to assess the effect of the test compound on the growth of the three human tumor cell lines. Cells were plated in 96-well flat-bottom microtiter plates at a cell density of 4000–20 000 cells per well. After a24 h recovery period to allow the cells to resume exponential growth the compounds were applied at 10 concentrations in half-logincrements in triplicates and treatment continued for 4 days. After 4 days of treatment, cells were next washed with 200 ml phosphate-buffered solution to remove dead cells, then 200 ml of a solution containing 7 mg/ml propidiumiodide and 0.1%(v/v) Triton X-100 were added to the wells. After an incubation period of 1–2 h at room temperature, fluorescence was measured using the Cytofluor 4000 microplate reader (Millipore, Schwalbach, Germany) (excitation l¼530 nm, emission l¼620 nm) to quantify the amount of attached viable cells. Pharmacological effects on cell proliferation and survival were expressed as Test/Control_100 (%T/C) values. On the basis of the T/C values, relative IC_{50} values were determined by non-linearregression (log[conc. of inhibitor] versus response (% T/C)) using the Graph Pad Prism analysis software. For calculation of mean IC_{50} values over the 3 cell lines as tested, the geometric mean was selected.

4. Results and discussion

4.1. Design of novel AR antagonists

2-Thioxo-5,5-dimethyl-imidazolidin-4-one is the common structural scaffold found as a core in known FDA approved AR antagonists Apalutamide (I) [18] and Enzalutamide (II) [19]. Keeping in mind the common structural scaffold, ten analogue molecules with structural features similar to reference compounds were designed. The central core was preserved, but the side arms were replaced with benzoxazole/benzothiazole and trifluoromethyl pyridine [20].Shape and electrostatic similarities of designed molecules were achieved to be similar to the ENZ (Table 1 and Figure 2c). We hypothesise that three-dimensional molecular shape and electrostatic features determine recognition by enzyme/receptor active site, contributing extensively to its binding affinity. Tanimoto shape similarity coefficient (TSSC) and Tanimotocolour similarity coefficient (TCSC) scores in the range of 0–1 were used to quantitatively compare and rank the similarity of shape and electrostatic features of designed molecules [21].Here, value of 1 indicates complete similarity and 0 indicates no similarity of shape (TSSC) and atom type (TCSC). The tanimoto combo (TC) is the sum of TSSC and TCSC. Indicates that the designed molecules having 0.57 to 0.68 TSSC score i.e. 57%–68% 3D shape similarity and 0.35 to 0.43 TCSC score i.e 35%–43% colour (atom to atom) similarity with Enzalutamide.

As shown in Figure 3a, c, designed molecule occupies the same shape and volume of Enzalutamide. Whereas, Figure 3b, representing pharmacophoric features of Enzalutamide like hydrogen bond donor (blue), hydrogen bond acceptor (red), ring (green) and hydrophobic region (yellow). Interestingly, ROCS studies demonstrate that the designed molecule features also match with these pharmacophoric requirements (Figure 3d). Benzoxazole/benzothiazole molecule overlaps with ring (green) and hydrogen bond acceptor region (red) [20]. However, trifluoromethyl pyridine overlay with ring (green) region but missed out-bond acceptor (red) and donor (blue) regions of Enzalutamide.

4.2. Chemistry

Syntheses of 5,5-dimethyl-3-(6-substituted-benzo[d]thia/oxazol-2-yl)-2-thioxo-1-(4-(trifluoromethyl)pyridin-2-yl)imidazolidin-4-one (**6a-j**) are described in Scheme 1. 2-isothiocyanato-6-susbstituted benzo[d]thiazole/benzo[d]oxazole (**2a-2j**) were prepared by reacting 2-aminobenzo[d]thiazole/benzo[d]oxazole with thiophosgene. Simultaneously, 2-methyl-2-(4-(trifluoromethyl)pyridin-2-ylamino)propanoate (**5**) was synthesized in two steps as follows, in first step, 2-Bromo-4-(trifluoromethyl)pyridine (**3**) reacted with 2-aminoisobutyric acid in presence of K_2CO_3 and CuCl to get 2-methyl-2-(4-(trifluoromethyl)pyridin-2-ylamino) propanoic acid (**4**). Then in the second step, product 4 was reacted with methyl iodide in presence of K_2CO_3 to obtain 2-methyl-2-(4-(trifluoromethyl)pyridin-2-ylamino)propanoate (**5**). While, in the last step, compound **2** and **5** were coupled in DMSO: Isopropyl acetate to get respective 5,5-dimethyl-3-(6-substituted-benzo[d]thia/oxazol-2-yl)-2-thioxo-1-(4-(trifluoromethyl)pyridin-2-yl)imidazolidin-4-one (**6a-j**).

4.3. Biological evaluation

In-vitro evaluation for determining the efficacy of novel Enzalutamide analogues (**6a - 6j**) against three different prostate cancer cell lines like

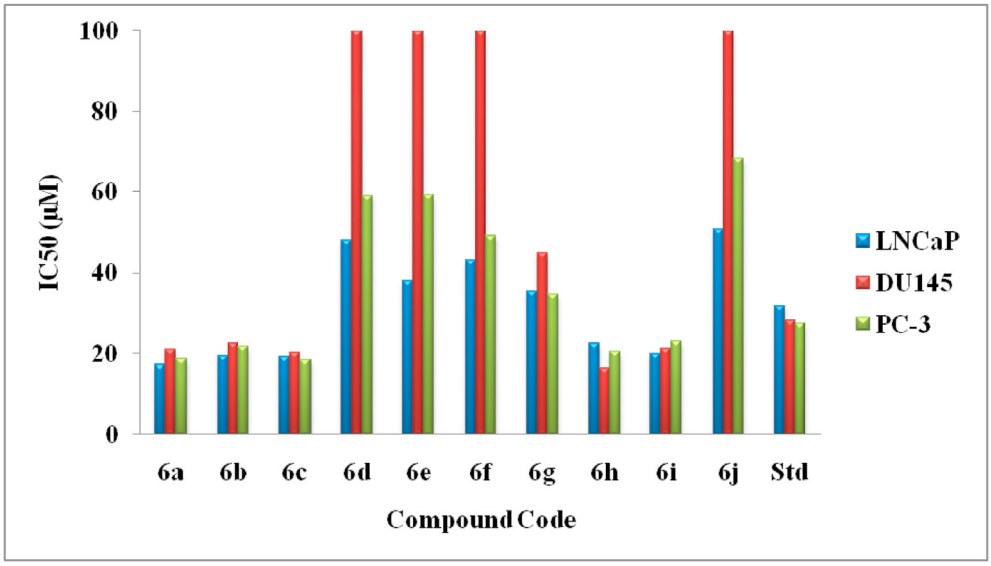

Figure 4. Antiproliferative activity of novel Enzalutamide analogues (**6a - 6j**).

DU-145, LNCaP and PC-3 were carried out. The results (Table 2) demonstrate that compound **6c** and **6h** are potent antiproliferative molecules. Compound 6c shows IC_{50} values of 20.31, 19.21 and 18.36 µM, whereas, compound **6h** had IC_{50} of about 16.50, 22.41 and 20.44 µM for the cell lines DU145, LNCaP and PC-3 respectively. The antiproliferative activity of these compounds was promising compared to the standard drug (Enzalutamide, IC_{50} = 28.20, 31.78 and 27.32 µM against the cell lines DU-145, LNCaP and PC 3 respectively). This in-vitro antiproliferative activity is also supported by the theoretical studies of binding affinity based on dock score of design molecules. It was found that two compounds, **6c** (Dock score = -8.49) and **6h** (Dock score = -8.46) exhibited similar binding affinity with the AR compared to the standard drug (Enzalutamide, Dock score = -10.49).

4.4. Molecular modelling studies

Molecular docking studies were performed with Schrodinger molecular modelling suite in the XP mode [22]. It demonstrated that designed molecules occupy similar pose and interactions similar to ENZ in the active site of AR earlier.

The drug molecule enzalutamide and its newly synthesised analogues were analysed initially by molecular docking studies. Then these molecules were subjected to the molecular dynamic simulations followed by MMGBSA calculations. The bicalutamide and enzalutamide are known as AR inhibitors. We designed and synthesised a series on analogues of these drugs. The compounds 6c and 6h have shown comparative activity in *in vitro* assays (Figure 4a). Compounds bicalutamide and enzalutamide are structural analogues, enzulatamide having a glycolyl thiourea nucleus similar to the test compounds; hence docking and molecular dynamics simulation for both drug molecules was performed. Docking of bicalutamide to the AR shows that; the drug molecule occupies the active site and interacts with the Trp741 and Leu876, which is similar to its interaction in the crystal structure (2AXA). Similarly, enzalutamide docks in AR (3V49) active site, and forms interactions with the residues Arg751 and His874 (Figure 5b, c).

To further evaluate the compounds, molecular dynamics studies performed in AMBER18 molecular modelling suite. The docked complexes, ligand **6a-j**, bicalutamide (BIC) and enzalutamide (ENZ) were validated to bind with the AR for 100 ns. The compounds were found to be stable throughout the simulation (Figure 6). ENZ, **6c** and **6h** were found to be stable during the period of simulation with slight variation in RMSD between 70 to 90 ns; Compound **6c** fluctuated between 15 to 45 ns and after that equilibrated to 1.5 Å, Compound 6h showed the RMSD between 1-2 Å for first 40 ns and later equilibrated to about 2 Å after 70 ns (Figure 7a). Figure 7b shows the superposition of ligands obtained from docking studies before the MDS. Rest of the ligands were also stable throughout the MD simulation with slight fluctuations between 70 to 90 ns (Figure 6). The structural changes were visibly studied, the docked complexes retained their position in all the cases, which is evident from their superposed structures before and after MDS (Figure 7). Compounds bound to the AR receptor crystal structure 2AXA retained their interactions with residues Trp741 and Leu876 (Figure 7b, c). In AR receptor crystal structure 3V49, the compounds 6c and 6h retained their interaction with the active site residues, Arg752 and His 874 (Figure 7e, f). The MM-PBSA/GBSA is a widely accepted tool for calculating the binding free energies of the biomolecular complexes. We performed these calculations to ascertain the interaction energies and stability of our ligand-protein complexes. AR-ENZ and AR-BIC were also studied along with the rest of the ten complexes as a measure of control. In this study, we selected all the 10000 frames from the MD trajectory. The binding energy and its components were obtained by the MM-GBSA methods for compounds ENZ, BIC, **6c** and **6h** are listed in Table 3; the rest of the information is provided in SI_table-1 [23].The individual components of the binding free energy calculations are van der Wall forces (vdW), electrostatic energy (EEL) as calculated by the MM force field, the electrostatic contribution to the solvation free energy calculated by GB (EGB), the electrostatic contribution to the solvation free energy calculated by PB (EPB) and Nonpolar solvation energy for GB and PB respectively (ENPOLAR) and nonpolar contribution to the solvation free energy (ESURF). As shown in Table 4, the compounds ENZ, **6c** and **6h** showed ΔG_{bind}values, -50.97, -35.23 and -35.74 kcal/mol^{-1} and -8 kcal/mol^{-1} respectively; indicates that ENZ has higher binding free energy, but compounds 6ca and 6h have comparable binding energies. In the docked complexes with AR crystal structure bound to Compound BIC, **6c** and **6d** showed binding energy of -45.11, -30.50 and -35.11 kcal/mol^{-1} respectively. In both cases, the van der Waal's contribution was high mainly due to the Ligand-protein complex's hydrophobic regions. The free energy calculations These results of binding free energy indicate that newly synthesised molecules do have good binding affinity to the AR but compared to the standard drug, they need further modifications to improve their binding efficiency.

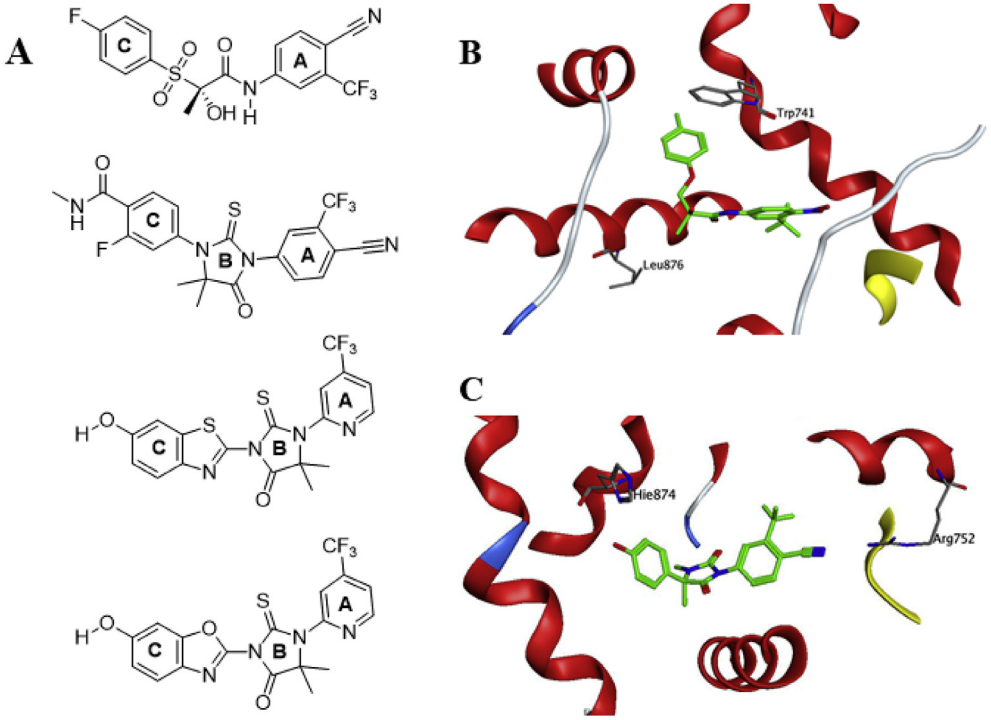

Figure 5. Molecular docking and dynamics simulations predict a novel binding mode for benzazole derivatives. **(A)** Structures of the anti-androgens bicalutamide (first from top), enzalutamide (second from top), and **6c** and **6h** oriented to highlight the molecules' common and discrete regions. The A-C annotation of the rings is indicated; **(B)**A magnified view of the docked structure of bicalutamide (green) in AR (PDB: 2AXA); (C) A magnified view of the docked structure of enzalutamide (green) in AR (PDB: 3V49).

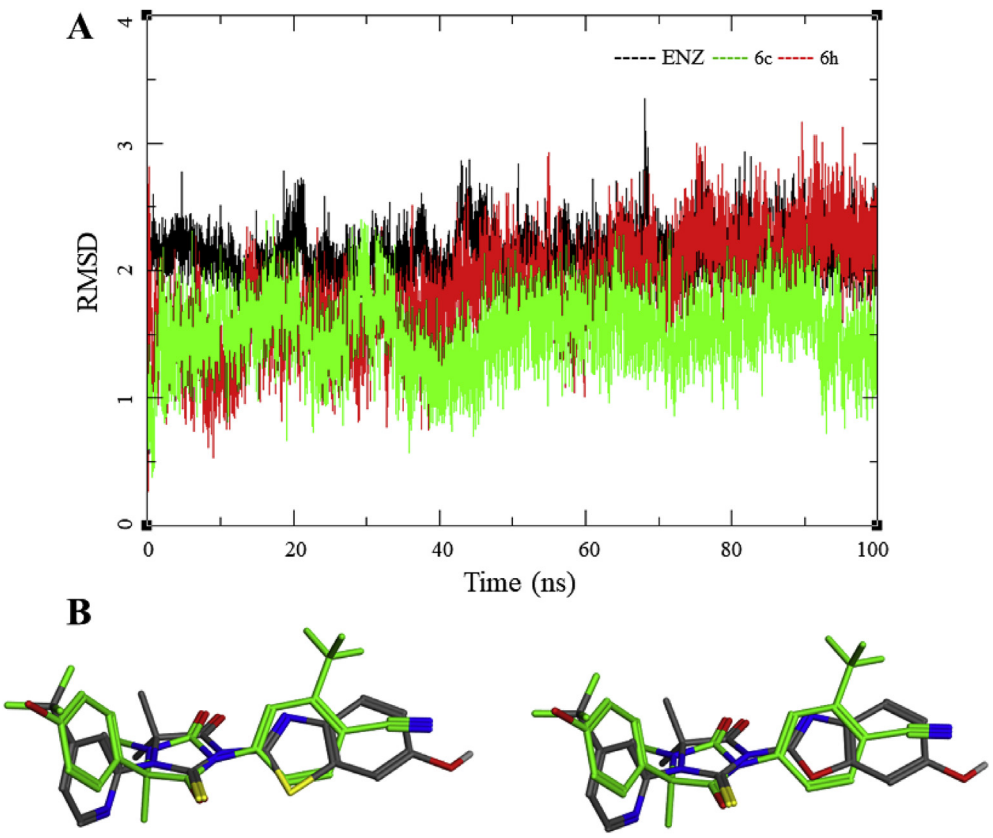

Figure 6. **(A)** Root mean square deviation (RMSD) in MDS for enzalutamide (ENZ), compound **6c** and **6h. (B)** The superposed structure obtained after molecular docking studies for ENZ-**6c** and ENZ-**6h** respectively.

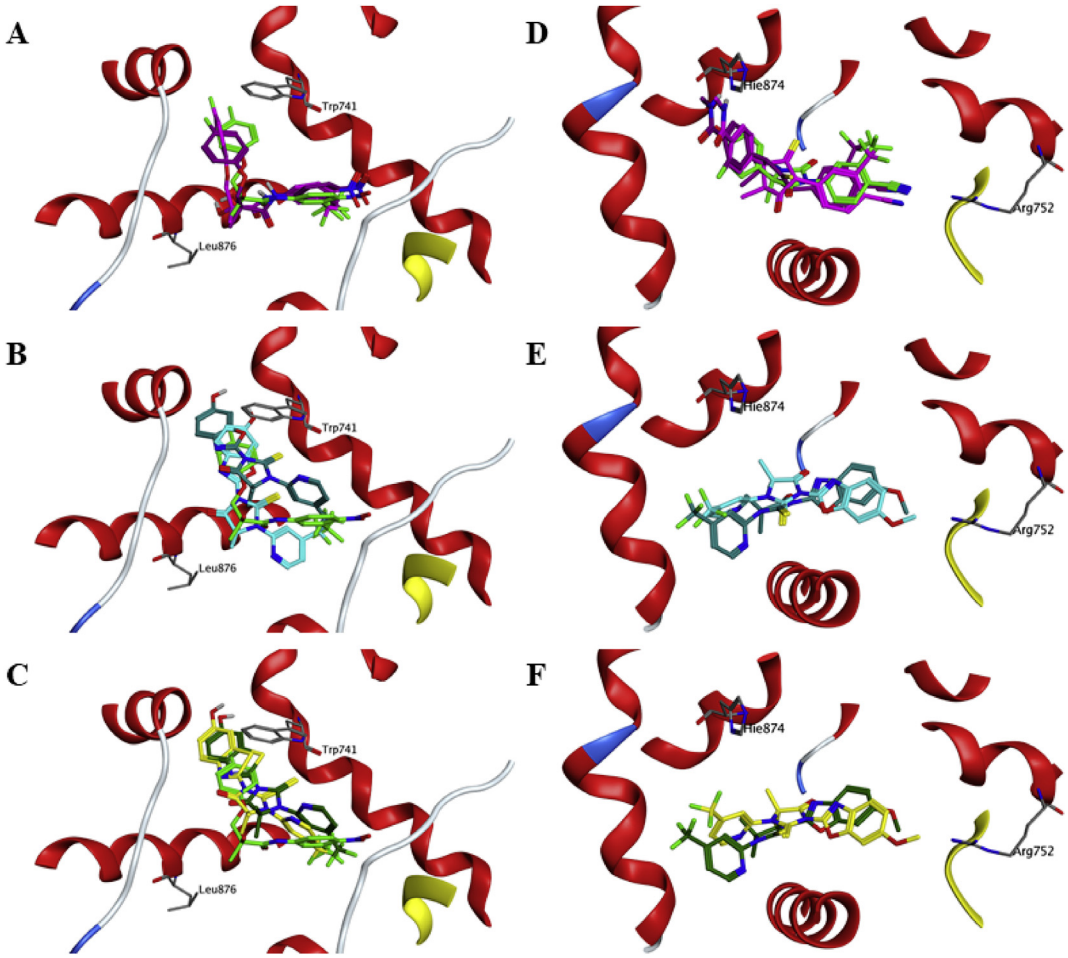

Figure 7. Molecular docking and dynamics simulations predict a novel binding mode for benzazole derivatives. **(A)** Bicalutamide cocrystal structure (green) in AR (PDB: 2AXA), magenta and purple are the initial and final conformation after molecular dynamics simulation for 100 ns; **(B)** Compound **6c** in complex with the AR in bicalutamide binding site, initial conformation (Cyan) and final conformation (dark blue) during the 100ns molecular dynamics simulation; **(C)** Compound **6h** in complex with the AR in bicalutamide binding site, initial conformation (yellow) and final conformation (dark green) during the 100ns molecular dynamics simulation; **(D)** Enzalutamide cocrystal structure (green) in AR (PDB: 3V49) magenta and purple are the initial and final conformation after molecular dynamics simulation for 100 ns; **(E)** Compound **6c** in complex with the AR in enzalutamide binding site, initial conformation (Cyan) and final conformation (dark blue) during the 100ns molecular dynamics simulation; **(F)** Compound **6h** in complex with the AR in enzalutamide binding site, initial conformation (yellow) and final conformation (dark green) during the 100ns molecular dynamics simulation.

Table 3. Binding free energy components for the protein-ligand complexes calculated by MM-GBSA analysis, all energies are in Kcal/mol with standard deviation in parenthesis.

Sr. No.	3V49			2AXA		
	Enzalutamide	6c	6h	Bicalutamide	6c	6h
MM/GBSA						
ΔE_{VDW}	-62.90 (2.8)	-58.20 (2.4)	-58.44 (2.6)	-53.33 (2.6)	-54.52 (2.6)	-56.16 (2.7)
ΔE_{ELE}	-19.98 (5.0)	-15.76 (2.8)	-14.66 (3.0)	-32.68 (6.0)	-15.81 (3.1)	-20.42 (3.2)
ΔG_{GB}	37.73 (3.4)	36.45 (2.4)	35.20 (2.6)	46.60 (5.3)	37.39 (2.7)	40.82 (2.5)
ΔG_{Surf}	-8.18 (0.1)	-7.59 (0.1)	-7.55 (0.1)	-7.76 (0.1)	-6.73 (0.1)	-6.88 (0.1)
ΔG_{bind}	-50.97 (3.2)	-35.23 (2.8)	-35.74 (3.0)	-45.11 (3.0)	-30.50 (2.8)	-35.11 (2.8)
Dock Score (Glide Score)	-10.49	-8.49	-8.46	-8.42	-7.50	-6.97

ΔE_{VDW} = van der Waals contribution from MM; **ΔE_{ELE}** = electrostatic energy as calculated by the MM force field; **ΔG_{GB}** = the electrostatic contribution to the solvation free energy calculated by GB; **ΔG_{Surf}** = solvent-accessible surface area; **ΔG_{Sol}** = solvation free energy; **ΔG_{gas}** = gas phase interaction energy; **ΔG_{bind}** = Binding free energy [12].

5. Conclusion

The quest of novel AR antagonist for the treatment of CRPC led to the design of novel molecules based on the shape and electrostatic similarity with Enzalutamide. ROCS results showed that the designed molecules have 58%–67% 3D shape similarity with Enzalutamide wherein compounds **6c** and **6h** showed highest TSSC scores (0.67). The in-vitro evaluation demonstrates that the compound **6c** and **6h** are promising

Table 4. Structural series of novel enzalutamide analogues.

Comp. no.	6a	6b	6c	6d	6e	6f	6g	6h	6i	6j
X	S	S	S	S	S	O	O	O	O	O
R_1	CH_3	OCH_3	OH	NO_2	Cl	CH_3	OCH_3	OH	NO_2	Cl

antiproliferative agents with IC_{50} 20.31 μM, 19.21 μM and 18.36 μM whereas, compound **6h** showed IC_{50} of 16.50 μM, 22.41 μM and 20.44 μM against DU-145, LNCaP and PC-3 prostate cancer cell lines respectively. It is remarkable that the novel compounds discovered in this study (**6c** and **6h**) are showing better in-vitro antiproliferative activity against prostate cancer cell lines compared to the standard compound (Enzalutamide) despite the less binding affinity. Also, the molecular docking, molecular dynamics and free energy calculations suggest the stability of the protein-ligand complex, which also indicates the affinity of the molecules to the receptor and comparable biological activity.

Declarations

Author contribution statement

Ritesh P. Bhole; Chandrakant G. Bonde: Conceived and designed the experiments; Performed the experiments; Analyzed and interpreted the data; Contributed reagents, materials, analysis tools or data; Wrote the paper.

Rupesh V. Chikhale: Conceived and designed the experiments; Performed the experiments; Contributed reagents, materials, analysis tools or data; Wrote the paper.

Ravindra D. Wavhale: Conceived and designed the experiments; Performed the experiments; Wrote the paper.

Fatmah Ali Asmary: Analyzed and interpreted the data.

Tahani Mazyad Almutairi: Performed the experiments; Analyzed and interpreted the data.

Hassna Mohammed Alhajri: Contributed reagents, materials, analysis tools or data.

Funding statement

This work was supported by AICTE, New Delhi, Research Promotion Scheme. (File No. 8-99/FDC/RPS (POLICY-l)/ 2019-20)

Data availability statement

Data included in article/supplementary material/referenced in article.

Declaration of interests statement

The authors declare no conflict of interest.

Additional information

No additional information is available for this paper.

References

[1] F. Bray, J. Ferlay, I. Soerjomataram, R. Siegel, L.A. Torre, A. Jemal, Prostate cancer statistics | World cancer research fund, CA. Cancer J. Clin. (2018).
[2] C. Huggins, C.V. Hodges, Studies on prostatic cancer i. the effect of castration, of estrogen and of androgen injection on serum phosphatases in metastatic carcinoma of the prostate, Cancer Res. (1941).
[3] E. Lee, A. Madar, G. David, M.J. Garabedian, R. DasGupta, S.K. Logan, Inhibition of androgen receptor and -catenin activity in prostate cancer, Proc. Natl. Acad. Sci. (2013).
[4] J. Zugazagoitia, C. Guedes, S. Ponce, I. Ferrer, S. Molina-Pinelo, L. Paz-Ares, Current challenges in cancer treatment, Clin. Ther. (2016).
[5] J. El-Amm, J.B. Aragon-Ching, The current landscape of treatment in non-metastatic castration-resistant prostate cancer, Clin. Med. Insights Oncol. (2019).
[6] S.S. Taneja, Re: increased survival with enzalutamide in prostate cancer after chemotherapy, J. Urol. (2013).
[7] K. Dalal, M. Roshan-Moniri, A. Sharma, H. Li, F. Ban, M. Hessein, M. Hsing, K. Singh, E. LeBlanc, S. Dehm, E.S. Tomlinson Guns, A. Cherkasov, P.S. Rennie, Selectively targeting the DNA-binding domain of the androgen receptor as a prospective therapy for prostate cancer, J. Biol. Chem. (2014).
[8] M. Korpal, J.M. Korn, X. Gao, D.P. Rakiec, D.A. Ruddy, S. Doshi, J. Yuan, S.G. Kovats, S. Kim, V.G. Cooke, J.E. Monahan, F. Stegmeier, T.M. Roberts, W.R. Sellers, W. Zhou, P. Zhu, An F876l mutation in androgen receptor confers genetic and phenotypic resistance to MDV3100 (Enzalutamide), Cancer Discov. (2013).
[9] R. Chikhale, S. Thorat, A. Pant, A. Jadhav, K.C. Thatipamula, R. Bansode, G. Bhargavi, N. Karodia, M.V. Rajasekharan, A. Paradkar, P. Khedekar, Design, Synthesis and pharmacological evaluation of pyrimidobenzothiazole-3-carboxylate derivatives as selective L-type calcium channel blockers, Bioorg. Med. Chem. 23 (2015).
[10] F. Nique, S. Hebbe, C. Peixoto, D. Annoot, J.M. Lefrançois, E. Duval, L. Michoux, N. Triballeau, J.M. Lemoullec, P. Mollat, M. Thauvin, T. Prangé, D. Minet, P. Clément-Lacroix, C. Robin-Jagerschmidt, D. Fleury, D. Guédin, P. Deprez, Discovery of diarylhydantoins as new selective androgen receptor modulators, J. Med. Chem. (2012).
[11] C.E. Bohl, D.D. Miller, J. Chen, C.E. Bell, J.T. Dalton, Structural basis for accommodation of nonsteroidal ligands in the androgen receptor, J. Biol. Chem. (2005).
[12] T.S. Lee, D.S. Cerutti, D. Mermelstein, C. Lin, S. Legrand, T.J. Giese, A. Roitberg, D.A. Case, R.C. Walker, D.M. York, GPU-accelerated molecular dynamics and free energy methods in Amber18: performance enhancements and new features, J. Chem. Inf. Model. (2018).
[13] R.P. Bhole, R.D. Wavhale, C.G. Bonde, R.V. Chikhale, Pharmacophore model and atom-based 3D quantitative structure activity relationship (QSAR) of human immunodeficiency virus-1 (HIV-1) capsid assembly inhibitors, J. Bio. Struct. Dyn. (2020).
[14] J. Wang, W. Wang, P. a Kollman, D. a Case, Antechamber, an accessory software package for molecular mechanical calculations, J. Am. Chem. Soc. (2001).
[15] D.J. Price, C.L. Brooks, A modified TIP3P water potential for simulation with Ewald summation, J. Chem. Phys. (2004).
[16] S. Bhowmick, R.D. Chorge, C.S. Jangam, L.D. Bharatrao, P.C. Patil, R.V. Chikhale, M.A. Islam, Identification of potential cruzain inhibitors using de novo design, molecular docking and dynamics simulations studies, J. Biomol. Struct. Dyn. (2019).
[17] S.A. Verekar, P.D. Mishra, E.S. Sreekumar, S.K. Deshmukh, H.H. Fiebig, G. Kelter, A. Maier, Anticancer activity of new depsipeptide compound isolated from an endophytic fungus, J. Antibiot. (Tokyo) (2014).
[18] K.N. Chi, N. Agarwal, A. Bjartell, B.H. Chung, A.J. Pereira de Santana Gomes, R. Given, Á. Juárez Soto, A.S. Merseburger, M. Özgüroğlu, H. Uemura, D. Ye, K. Deprince, V. Naini, J. Li, S. Cheng, M.K. Yu, K. Zhang, J.S. Larsen, S. McCarthy, S. Chowdhury, Apalutamide for metastatic, castration-sensitive prostate cancer, N. Engl. J. Med. (2019).
[19] I.D. Davis, A.J. Martin, M.R. Stockler, S. Begbie, K.N. Chi, S. Chowdhury, X. Coskinas, M. Frydenberg, W.E. Hague, L.G. Horvath, A.M. Joshua, N.J. Lawrence, G. Marx, J. McCaffrey, R. McDermott, M. McJannett, S.A. North, F. Parnis, W. Parulekar, D.W. Pook, M.N. Reaume, S.K. Sandhu, A. Tan, T.H. Tan, A. Thomson, E. Tu, F. Vera-Badillo, S.G. Williams, S. Yip, A.Y. Zhang, R.R. Zielinski, C.J. Sweeney, Enzalutamide with standard first-line therapy in metastatic prostate cancer, N. Engl. J. Med. (2019).
[20] R. Chikhale, S. Thorat, R.K. Choudhary, N. Gadewal, P. Khedekar, Design, Synthesis and anticancer studies of novel aminobenzazolyl pyrimidines as tyrosine kinase inhibitors, Bioorg. Chem. (2018).
[21] S. Kearnes, V. Pande, ROCS-derived features for virtual screening, J. Comput. Aided Mol. Des. (2016).
[22] R. Chikhale, S. Menghani, R. Babu, R. Bansode, G. Bhargavi, N. Karodia, M.V. Rajasekharan, A. Paradkar, P. Khedekar, Development of selective DprE1 inhibitors: design, Synthesis, crystal structure and antitubercular activity of benzothiazolylpyrimidine-5-carboxamides, Eur. J. Med. Chem. (2015).
[23] M.A. Islam, T.S. Pillay, Pharmacoinformatics-based identification of chemically active molecules against Ebola virus, J. Biomol. Struct. Dyn. (2018).
[24] R.P. Bhole, K.P. Bhusari, Synthesis and antitumor activity of (4-hydroxyphenyl) [5-substituted alkyl/aryl)-2-thioxo-1,3,4-thiadiazol-3-yl]methanone and [(3,4-disubstituted)-1,3-thiazol-2ylidene]-4-hydroxybenzohydrazide, Med. Chem. Res. (2010).